Experimental Investigation for Capturing Liquid Free Surface Elevation in an Externally Induced Tank

M. Eswaran[1], Ujjwal K. Saha[2]

[1]Structural and Seismic Engineering Section, Reactor Safety Division, Bhaba Atomic Research Centre, Trombay, Mumbai – 400 085, India

[2]Department of Mechanical Engineering, Indian Institute of Technology Guwahati, Guwahati-781 039, India

[1] eswaran@barc.gov.in; [2] saha@iitg.ernet.in

Abstract

This paper pays attention to finding the free surface elevation during liquid sloshing at low excitation frequency. Experiments have been conducted at low frequency ratios to find the free surface elevation and the obtained results are reported here. The liquid behavior is captured by means of a video camera and the free surface oscillations of liquid at different excitation frequencies calculated by the image processing technique. The liquid height is observed by the intensity variation of the interface between the air and liquid. The location of maximum gradient has been considered as interface. The effects of excitation amplitude, frequency and liquid fill level have been studied.

Keywords

Liquid Sloshing; Image Processing; Free Surface

Introduction

The knowledge of natural frequencies for the liquid free surface is important in the design of liquid tanks subjected to different types of excitation. The dynamic behavior of a free liquid surface depends on the type of excitation and its frequency content. Excitation with frequencies in the vicinity of the lowest natural frequencies of the liquid motion is of primary practical interest. Civil engineers and seismologists have been studying liquid sloshing effects on large dams, oil tanks and elevated water towers under ground motion. Sloshing phenomenon is one of the major concerns in the design of liquid storage tanks undergoing ground excitation (Maleki and Ziyaeifar, 2008). Experimental studies can provide very useful and reliable results for some cases. However, they are generally very expensive. Moreover, there is a lack of high quality experimental data in the area of liquid sloshing (Akyildiz and Unal, 2005). Sloshing can be broadly classified into two types, namely self-induced sloshing and externally induced sloshing, based on how sloshing is generated inside its container. The main difference is that, in self-induced sloshing, the container is immobile whereas, in externally induced sloshing, the container will move owing to external disturbances. Several investigations on self-induced sloshing (Hu *et al.* 1999, Okamoto *et al.* 1991, Saga *et al.* 2000, Singh *et al.* 2006, Nasar *et al.* 2009) in a rectangular tank with circulating flow have been conducted experimentally and numerically in the past 20 years (Takizawa *et al.* 1992, Okamoto *et al.* 1993, Fukaya *et al.* 1996). Most of the studies on sloshing were limited to self-induced excitations. In the case of externally induced sloshing, an external force such as an earthquake or a sudden brake on a moving container vehicle acts as the excitation source for sloshing. The effect of sloshing in a moving liquid container causes safety and comfort issues such as undesirable forces on brake systems in liquid carrying tankers like LNG (Graczyk *et al.* 2006, Lee *et al.* 2007), high impact loads upon the containment system and structural parts. Further, under earthquake conditions, it creates fatigue, safety problems in nuclear reactors and power generating plants (Kimura *et al.* 1995). Detailed review of literatures can be found in Ibrahim (2005) and in Eswaran and Saha (2011).

Experimental Plan

In this investigation, the liquid behavior in an externally induced tank is captured by means of a video camera and the free surface oscillations of liquid at different excitation frequencies calculated by image processing technique. Finally, the statistical analysis is performed to show the probability density and power spectral density of signal.

Experimental Facilities and Procedures

Figure 1 shows the schematic diagram of the experimental set-up, details of which have already been reported by Eswaran *et al.* (2009) and Panigrahy *et al.* (2009). The partially filled liquid tank of size 600 mm x 600 mm x 600 mm is attached to a shaking table (915 mm x 930 mm) which can be moved to and fro by a crank arrangement and is driven by a DC motor (rated 1440 RPM, 220 V, 1 HP). As the required frequency of oscillation is too low, therefore, a rectifier-cum-controller is used to obtain the desired frequency of oscillation. The controller that converts the alternating current to direct current and feeds it to the DC motor with appropriate regulation is connected with the DC motor. It contains a full wave rectifier, which converts the 220V AC-1ϕ supply to 220V DC.
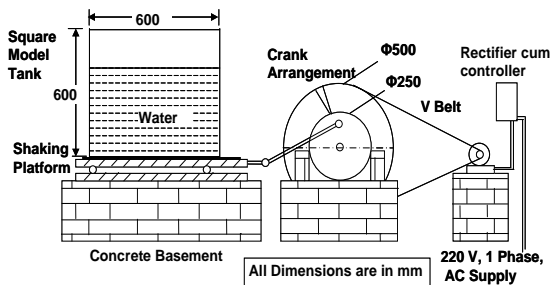

FIG. 1 BASIC EXPERIMENTAL SET-UP

The crank arrangement is used in the set-up to transform the rotary motion to reciprocating motion which connects the DC motor and the platform of the shaking table. The water is used as a working fluid in the experiments. A video camera (Sony DCR-SR 300 Handy cam Camcorder) is screwed onto an adjustable beam which is attached to the shaking platform with its lens focusing on the liquid free surface at the left corner of the tank as shown in Figure 2. The adjustable beam is moved up or down until a suitable slot is reached so that the camera focuses only on the liquid during its entire motion.
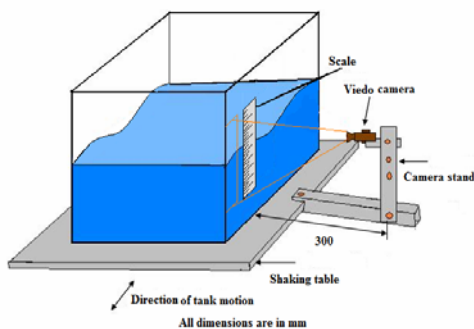

FIG.2 CAMERA ARRANGEMENT IN THE SET-UP FOR FINDING THE FREE SURFACE ELEVATION

The camera is held at a distance of 300 mm away from the liquid free surface and focuses on the water free surface. Initially, the relation between the pixel and millimeter has been found by still images. The camera is then ready to capture the images of the air-water interface as shown in Figure 3. After adding a coloring agent (navy blue) in the liquid, an excellent contrast between the liquid and the white marker particles is obtained that gives a superior image quality with lesser noise. The motor is allowed to rotate whose speed can be varied using a speed controller. The speed of the motor is kept sufficiently low so that the sloshing occurs without much turbulence. The tank can be filled to any desired level and a scale attached to the side wall of the tank gives the height. The experiments have been conducted by varying the frequencies and the h_s/L ratio of the tank for different case studies.
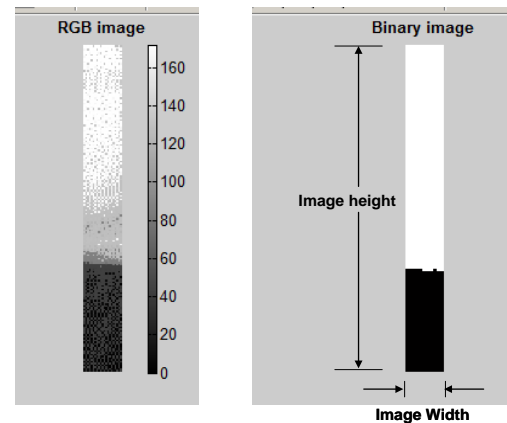

FIG.3 CONVERSION OF RGB IMAGE INTO BINARY IMAGE

Interface Location Technique for Capturing Free Surface Elevation

The luminance contrast between the liquid and the air which indicates the location of the interface is determined by maximum intensity gradient method. The location of maximum gradient is considered as interface as described by Law *et al.* (1999) and Eswaran *et al* (2011). The videos captured by the video camera are then transferred to the computer, and further image analysis is carried out. The liquid height is observed by the intensity variation of the interface between the air and liquid. The intensity gradient at each point has been calculated. The location of maximum gradient has been considered as interface. The movement of interface can be analyzed by cross-correlation between these matrices. The free surface oscillations are plotted for different excitation frequencies. Figure 4 shows the typical pixel intensity

variation along a vertical line cutting across the interface region. The movement of the interface can be tracked by analyzing its displacement between two successive images.
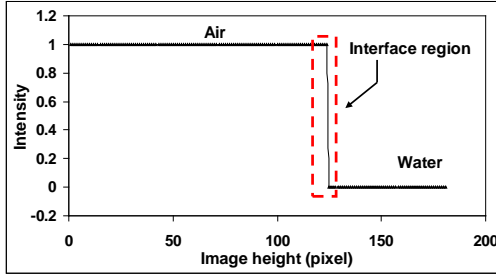

FIG.4 INTENSITY VALUES FOR BINARY IMAGE

All images are then available in the form of a vertical location matrix. The movement of interface can be analyzed by cross-correlation between these matrices. The standard deviation of extracted vertical locations denotes the interface fluctuation with time and the mean value gives the mean fluctuation for the corresponding excitation frequency and h_s/L ratio.

Tests to Ensure the Accuracy of Experimental Results

Depending upon the type of liquid, nature of external disturbances on the tank, tank shape and h_s/L ratio, the free liquid surface can experience different motions like simple planar, non-planar, rotational, irregular beating, symmetric, asymmetric, quasi-periodic and chaotic (Ibrahim, 2005). The amplitude of slosh, in general, depends upon the nature, amplitude and frequency of the tank motion, liquid-fill depth, liquid properties and tank geometry (Pal *et al.* 2002, Akyildiz and Unal, 2006). As the rectangular tank oscillates, different sloshing waves are created depending on the liquid depth and frequency of oscillations. In this study, the problem was restricted to liquid sloshing in a rectangular tank under surge (movement of tank only in horizontal direction) oscillations. The dynamic tank velocity (V_t) can be determined from the following equation,

$$V_t = -A_t \omega \cos(\omega t) \tag{1}$$

where A_t is the tank excitation amplitude and ω is the oscillation frequency. The amplitude of the tank excitation is 100 mm. For a given rectangular prismatic tank, the natural frequencies of the fluid depending on the fill depth are given by,

$$\omega_n{}^2 = g \frac{n\pi}{L} \tanh\left(\frac{n\pi}{L}d\right) \tag{2}$$

where L and d are the tank width and water depth respectively and n is the mode number (Akyildiz and Unal, 2005). In Table 1, different combination of liquid h_s/L ratio, excitation frequency and excitation amplitude are shown for a total of thirty six cases. It is to be noted that at higher frequency, the turbulence level becomes higher. If the frequency of the tank motion is close to the natural frequency of the liquid, large sloshing amplitude occurs. Since the liquid elevation is calculated through image processing, the more turbulence of liquid should be avoided which will induce noises while processing. Thus, all the experiments have been conducted at low frequencies only.

Uncertainty Analysis

Uncertainty is a quantification of the doubt about the measured result. The maximum possible uncertainty is estimated from the minimum value of quantity measured and accuracy of the measuring system. The maximum error calculated while measuring the excitation frequency is 0.014 cycle/sec. The experiments are repeated and are found consistent. The detailed error analysis is discussed in Appendix A.

Repeatability of Experiment

In the experimental plan as mentioned in Table 1, the set 5 was used to the check repeatability of experiments. The repeatability of the slosh phenomenon was investigated by running the same experiment several times. The test is conducted by plotting the height versus time for case numbers from 37 to 41 which is sketched in Figure 5. It is seen that the measurements are very close to each other. To get a measure of how close the experiments are, the standard deviation is calculated for each time instant. The calculation of the standard deviation $\sigma(t)$ is given by

$$\sigma(t) = \sqrt{\frac{1}{4}\sum_{i=1}^{5}(\zeta(t) - m(t))^2} \tag{3}$$

$$m(t) = \frac{1}{5}\sum_{i=1}^{5}\zeta_i(t) \tag{4}$$

where ζ_i is the measured surface elevation of experiment $i = 1,2 . . . ,5$ and $m(t)$ is the average of all experiments. The standard deviation $\sigma(t)$ is shown in Figure 6. The standard deviation is found smaller as

compared to the measured value, thus showing the repeatability of the tests.
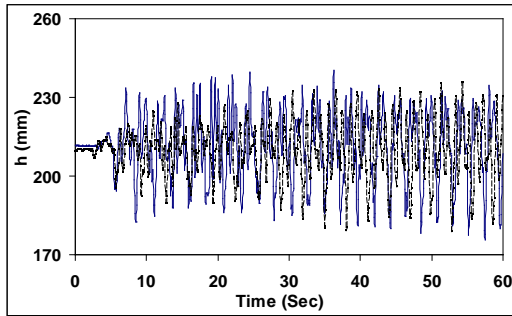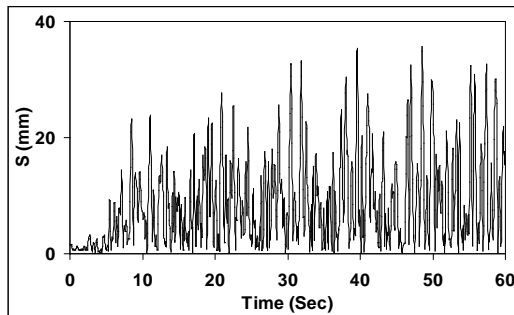

FIG.5 REPEATABILITY OF TEST (CASE-37 to 41)

FIG. 6 STANDARD DEVIATION OF EXPERIMENTS (CASE-37 to 41)

Validation with Wave Height Gauge

Wave elevation can also be measured using wave height gauge. As shown in Figures 7 and 8, three distinct marks viz., upper, lower and midpoint are made on the probe wire for convenience. Initially, the lower mark is set to immerse in the tank liquid and the liquid level is adjusted to coincide with the middle mark. The difference in permittivity between water and air is used to measure the surface elevation in a moving tank. Then the gauge results are compared with the results obtained from interface location technique as shown in Figure 9. When the surface is oscillating, a thin layer of liquid is formed on the package wall. This thin layer of liquid moves down much slower than the surface of the liquid. However, the result matches well with allowable accuracy.
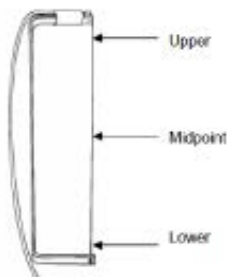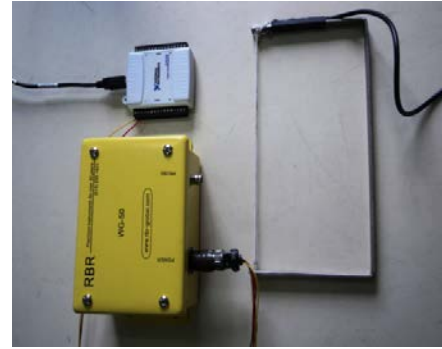

FIG.7 WAVE PROBE

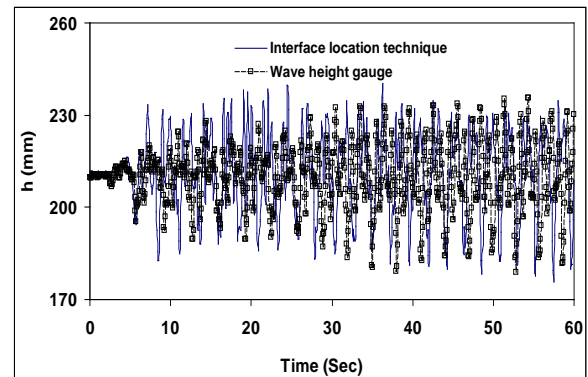FIG.8 PERSPECTIVE VIEW OF WAVE PROBE AND ANALOGG TO DIGITAL CONVERTER

FIG.9 TANK 600 x 600 x 600 mm, FL=200 mm, FR=0.6, EXCITATION AMPLITUDE=60 mm

Comparison of Experimental and Numerical Results

In this section, the experimental results for two different frequency ratios are compared with the numerical simulation results. Numerical simulation procedures and results have already been reported by Eswaran and Saha (2009, 2010). A fully non-linear model for idealized 3-D waves in a numerical wave tank has been developed. A sigma (σ) transformation is used to map the liquid domain onto a rectangle, such that the moving free surface in the physical plane becomes a fixed line in the computational mapped domain. The fourth order central difference scheme and the Gauss–Seidel point successive over-relaxation iterative procedure are used to capture the free surface wave profiles and free surface elevation plots of the fluid domain.

The free surface elevation for both simulated and experimental results is compared during the motion of tank and a minor discrepancy has been observed. It can be observed from Figures 10 and 11 that both experimental and numerical results indicates the presence of a single traveling wave. Two cases are considered for such a validation by choosing two different frequency ratios. In the both cases, the

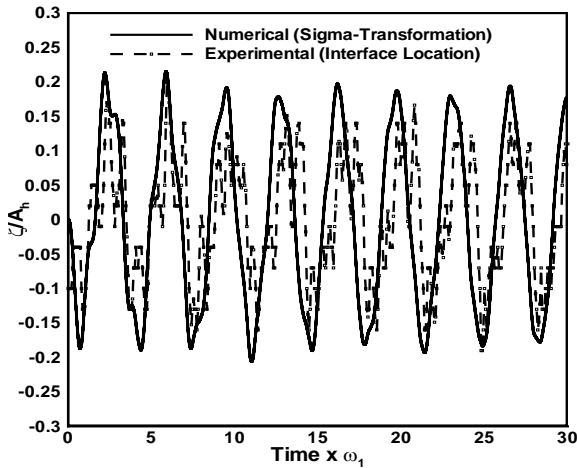excitation amplitude and the fill ratio (h_s/L=0.5) remains constant.

FIG. 10 FREE SURFACE ELEVATION FOR CASE-19

(FR=27.4 %; h_s/L =0.5; EA=30 mm)

The excitation amplitude (EA) value has been chosen as 30 mm since better results can be expected with low excitation amplitude for the present experimental and numerical works. When the results are closely examined, one can observe that the numerical results clearly over scoop the experimental results for the case of high frequency ratio (Figure 12). But when the frequency ratio is low, the crest and trough points in both results are matched well.
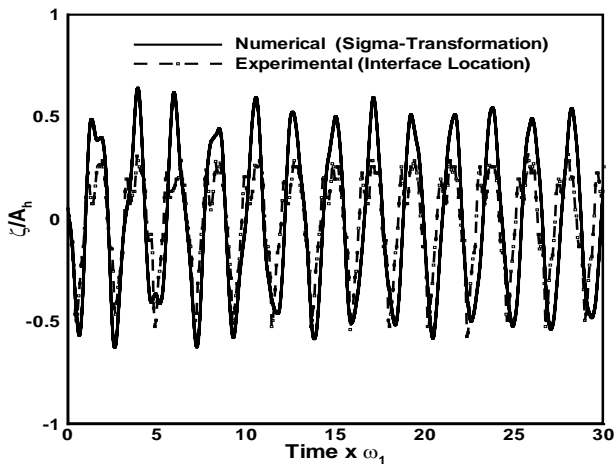

FIG.11 FREE SURFACE ELEVATION FOR CASE-20

(FR=36.6 %; h_s/L =0.5; EA=30 mm)

Results and Discussion of Free Surface Elevation

Effect of Excitation Amplitude

As the rectangular tank oscillates, different sloshing waves are created depending on the liquid depth and frequency of oscillations. These waves are asymmetric

and at large amplitude the tank excitations are combined with the travelling waves. Liquid heights for different frequency ratios under low amplitude excitation (EA=30 mm) for cases 11 and 12 as per Table 1 are shown in Figures 12 and 13 respectively. For the case of low amplitude excitation, the liquid height reaches the steady level quickly. It is observed that the slosh amplitude follows a sinusoidal pattern which means the initial increase of slosh amplitude with the increase in applied frequency and thereafter it decreases and again with the increase in external frequency the slosh amplitude increases. This is because of the sinusoidal nature of applied external excitation.
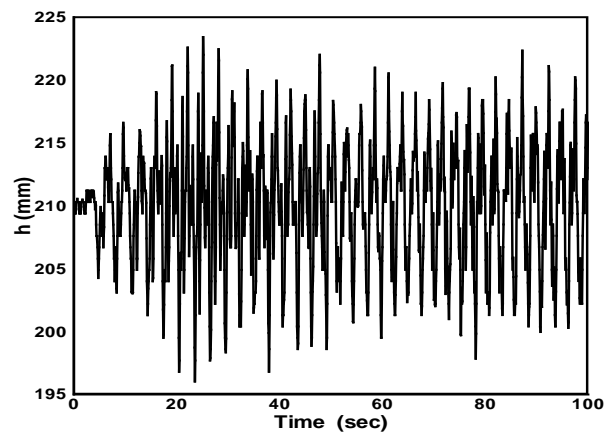

FIG.12 FREE SURFACE ELEVATION FOR CASE-11

(FR=39 %; h_s/L =0.35; EA=30 mm)

As the amplitude of excitation is increased (EA=100 mm), the liquid responds violently related to the fluid motion that occurs due to the occurrence of turbulence, hydraulic jump, wave breaking and 3-D effects. Figure 14 shows the liquid height for different frequencies at 100 mm excitation amplitude. It has been observed that the wave amplitude grows initially with the time up to a certain time period. After reaching this period, the wave amplitude remains constant and enters the fully developed region. In other words, in the first phase, the wave amplitude rises slowly from mean level up to certain period whereas in the second phase, a uniform oscillation can be observed. Similar trend is noticed for rest of the cases (case-28 to case-36) in set 4 experiments of Table 1. Free surface oscillation or the instantaneous wave height (h) for first phase (i.e., 0 to 20 seconds) and for second phase (i.e., 100 to 120 seconds) at tank left wall for case-28 is shown in Figures 15 (a) and (b) respectively, and their corresponding wave phase plane diagrams are depicted in Figure 16 (a) and (b). In each case, the instantaneous wave height is plotted for first phase and second phase time periods.
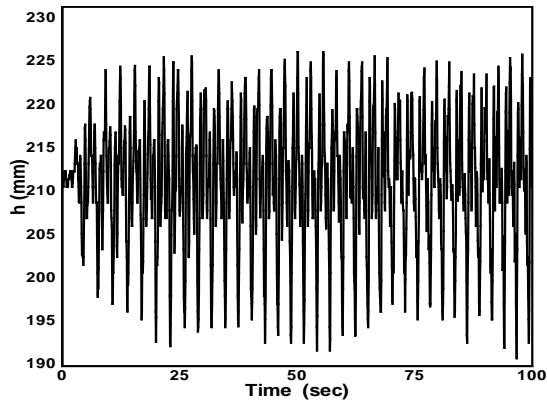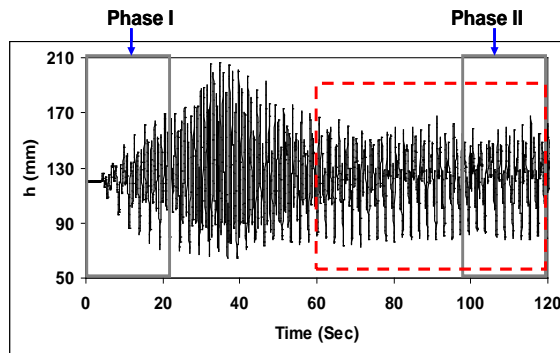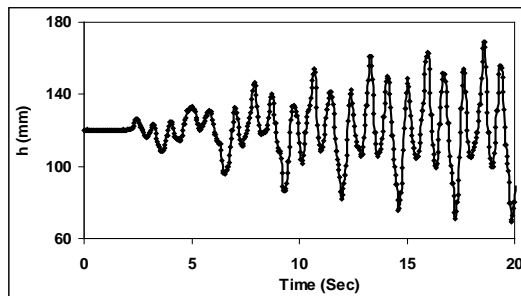
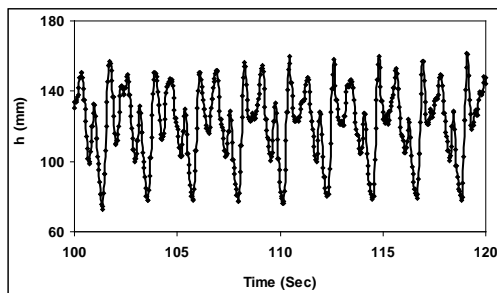FIG.13 FREE SURFACE ELEVATION FOR CASE-12

(FR=49 %; h_s/L =0.35; EA=30 mm)

FIG.14 FREE SURFACE ELEVATION FOR CASE-28

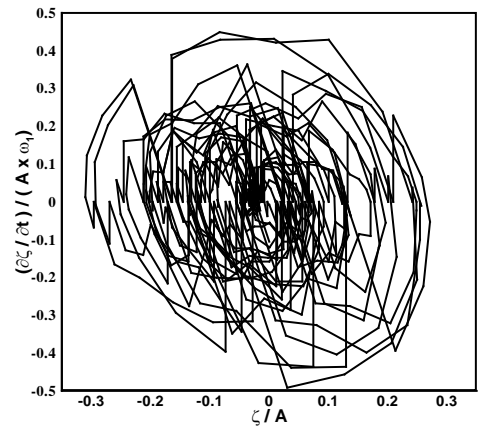(FR=29 %; h_s/L =0.35; EA=100 mm)

(a)

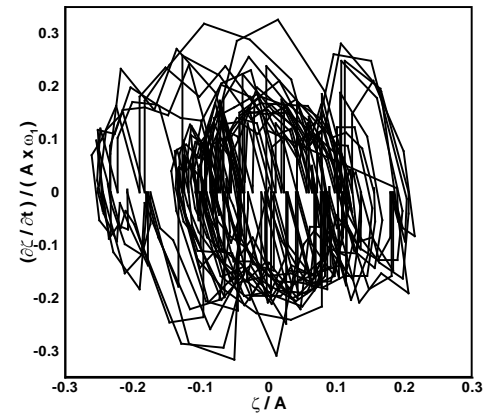(b)

FIG.15 FREE SURFACE ELEVATION FOR CASE-28

(a) Phase I; (b) Phase II.

(a)

(b)

FIG.16 PHASE PLANE DIAGRAM FOR CASE-28

(a) Phase I; (b) Phase II.

Effect of Excitation Frequency and Fill Level

As the tank moves, it supplies energy to sustain the liquid motion. The four possible types of waves are standing wave, traveling wave, hydraulic jump and a combination of these. Figures 17 and 19 show the effect of excitation frequency and effect of fill level. As the frequency increases, the standing wave transforms into a train of traveling waves of very short length, and the hydraulic jump occurs near first mode natural frequency. Further, with increase of frequency, the standing wave transforms into a train of traveling waves of very short length. Hydraulic jump, usually, takes place due to a small disturbance and appears over a range of frequencies near the resonant frequency (Akyildiz and Unal, 2005). With further increase in frequency, the jump will pass into a solitary wave. For deeper liquid, sloshing near the resonance is characterized by the formation of large amplitude standing waves. These waves are asymmetric in nature, and at large amplitude, tank excitations may be combined with the traveling waves.

TABLE 1 DETAILS OF THE EXPERIMENTAL PARAMETERS

Set No.	Case	Excitation Amplitude (EA)	Fill Level (FL)		Excitation Frequency (ω_h)		First Mode Natural Frequency (ω_1)	FR $(\omega_n/\omega_1)\times100$
		mm	mm	h_s/L ratio	cycle/sec	rad/sec	rad/sec	%
Set 1	1	30	120	0.2	0.3	1.885	5.34835	35.24
	2	30	120	0.2	0.4	2.513	5.34835	46.98
	3	30	120	0.2	0.5	3.142	5.34835	58.74
	4	40	120	0.2	0.3	1.885	5.34835	35.24
	5	40	120	0.2	0.4	2.513	5.34835	46.98
	6	40	120	0.2	0.5	3.142	5.34835	58.74
	7	60	120	0.2	0.3	1.885	5.34835	35.24
	8	60	120	0.2	0.4	2.513	5.34835	46.98
	9	60	120	0.2	0.5	3.142	5.34835	58.74
Set 2	10	30	210	0.35	0.3	1.885	6.41167	29.40
	11	30	210	0.35	0.4	2.513	6.41167	39.19
	12	30	210	0.35	0.5	3.142	6.41167	49.00
	13	40	210	0.35	0.3	1.885	6.41167	29.40
	14	40	210	0.35	0.4	2.513	6.41167	39.19
	15	40	210	0.35	0.5	3.142	6.41167	49.00
	16	60	210	0.35	0.3	1.885	6.41167	29.40
	17	60	210	0.35	0.4	2.513	6.41167	39.19
	18	60	210	0.35	0.5	3.142	6.41167	49.00
Set 3	19	30	300	0.5	0.3	1.885	6.86364	27.46
	20	30	300	0.5	0.4	2.513	6.86364	36.61
	21	30	300	0.5	0.5	3.142	6.86364	45.77
	22	40	300	0.5	0.3	1.885	6.86364	27.46
	23	40	300	0.5	0.4	2.513	6.86364	36.61
	24	40	300	0.5	0.5	3.142	6.86364	45.77
	25	60	300	0.5	0.3	1.885	6.86364	27.46
	26	60	300	0.5	0.4	2.513	6.86364	36.61
	27	60	300	0.5	0.5	3.142	6.86364	45.77
Set 4	28	100	210	0.35	0.3	1.885	6.41167	29.39
	29	100	210	0.35	0.35	2.199	6.41167	34.29
	30	100	210	0.35	0.4	2.513	6.41167	39.19
	31	100	210	0.35	0.5	3.142	6.41167	49.00
	32	100	120	0.2	0.3	1.885	5.34835	35.21
	33	100	120	0.2	04	2.513	5.34835	47.26
	34	100	180	0.3	0.3	1.885	6.15000	30.59
	35	100	180	0.3	0.4	2.513	6.15000	40.81
	36	100	240	0.4	0.3	1.885	6.60861	28.52
Repeatability test								
Set 5	37	30	300	0.5	0.8	5.0265	6.86364	73.23
	38	30	300	0.5	0.8	5.0265	6.86364	73.23
	39	30	300	0.5	0.8	5.0265	6.86364	73.23
	40	30	300	0.5	0.8	5.0265	6.86364	73.23
	41	30	300	0.5	0.8	5.0265	6.86364	73.23

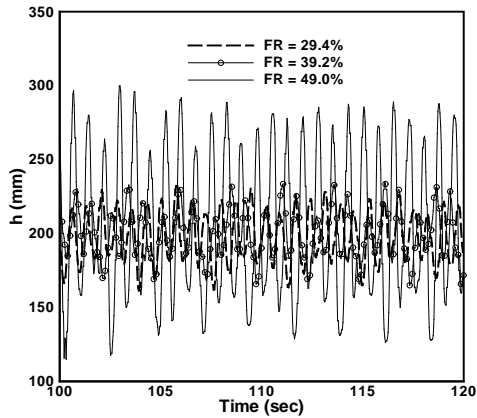(H = Height of the test tank; hs = Fill water level; L= Length of the tank)

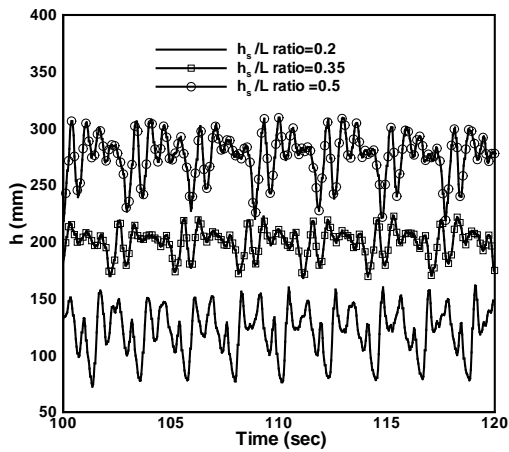FIG.17 EFFECT OF FREQUENCY FOR CASES – 13, 14 and 15
(h_s/L =0.35; EA=40 mm)

FIG. 18 EFFECT OF FILL LEVEL FOR CASES – 8, 17 and 27
(FR ≈ 49; hs/L =0.35; EA=30 mm).

Figure 19 shows the bar chart representation of maximum and minimum wave heights for case 1 through 4. The maximum and minimum wave height for first phase and second phase is represented as Imax, Imin and Smax, Smin respectively. It shows that the maximum wave height increases and minimum wave height decreases while increasing the frequency.
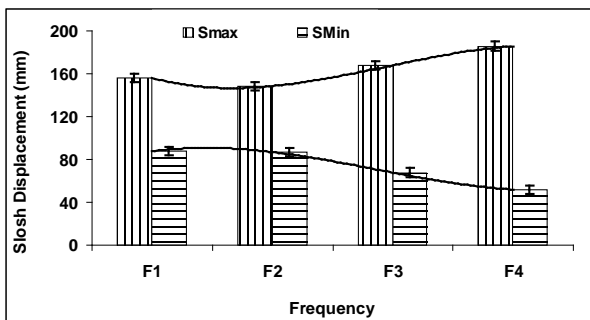

FIG. 19 BAR CHART REPRESENTATION OF MAXIMUM AND MINIMUM SLOSH DISPLACEMENT WITH FREQUENCY FOR CASES – 28 to 31(h_s/L =0.35; EA=100 mm). (F1 – 1.885 rad/sec, F2 – 2.199 rad/sec, F3 – 2.513 rad/sec, F4 – 3.142 rad/sec).

Spectra of Wave Elevation

The spectra of a wave elevation are computed by the Fast Fourier Transform (FFT) as shown in Figure 20, where S is the wave elevation spectrum. Figure 20 shows the spectra of wave elevations at the tank left corner. It causes peaks in the power spectra and more peaks appear at different frequencies. The sloshing waves have been analyzed with the probability density and energy spectrum.
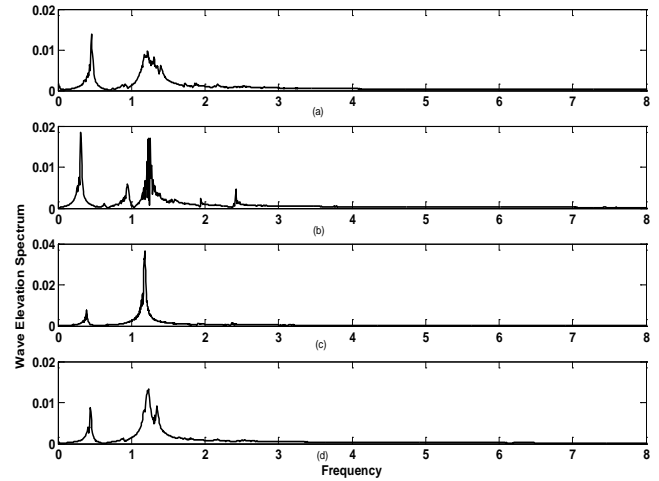

FIG.20 POWER SPECTRA OF WAVE ELEVATION AT THE TANK LEFT CORNER: (a) CASE-28; (b) CASE-29;

(c) CASE-30; and (d) CASE-31

Conclusions

This paper is devoted to presenting the experimental procedure for finding the free surface elevation in a moving rectangular tank. The liquid free surface behavior at low frequency oscillation has been elaborately studied from experiments. Initially, the history of wave or long term behavior of free surface oscillation (0 to 120 seconds) is observed. Thereafter, to study in detail, two time phase periods are focused and instantaneous wave heights are plotted for each case. It has been observed that the wave amplitude grows initially with the time up to a certain time period. After reaching this period, the wave amplitude remains constant and enters the fully developed region. It is found that the maximum wave height increases with an increasing frequency, while the minimum wave height decreases with increasing frequency. It also causes the peaks in the power spectra to become larger and encourages more peaks to appear at different frequencies. The sloshing waves have been analyzed with the probability density and energy spectrum. It is clear that the trend of deviation of wave height increases with an increase in frequency.

This suggests that a stronger nonlinearity gives rise to the increase of the deviation. It is interesting to note that such an increase seems to indicate a fairly linear trend with frequency. Finally, the experimental data have been compared with the results obtained from the numerical simulation.

REFERENCES

Akyildiz, H. and Unal, E. "Experimental Investigation of Pressure Distribution on Rectangular Tank due to Sloshing." Ocean Engineering, 32, 1503–1516, 2005.

Akyildiz, H. and Unal, N. E., "Sloshing in a Three Dimensional Rectangular Tank: Numerical Simulation and Experimental Validation." Ocean Engineering, 33(16), 2135–2149, 2006.

Eswaran, M., Saha, U. K., and Maity, D. "Effect of Baffles on a Partially Filled Cubic Tank: Numerical Simulation and Experimental Validation." Computers and Structures, 87(3–4), 198–205, 2009.

Eswaran, M., and Saha, U. K., "Low Steeping Waves Simulation in a Vertical Excited Container Using σ-Transformation." Paper No. OMAE2009–80248, 28th International Conference on Ocean, Offshore and Arctic Engineering, May 31–June 5, Honolulu, Hawaii, USA, 2009.

Eswaran, M., and Saha, U. K., "Waves Simulation in an Excited Cylindrical Tank Using σ Transformation." ASME International Mechanical Engineering Congress and Exposition, Paper No. IMECE2010–39752, November 12–18, Vancouver, Canada, 2010.

Eswaran, M., and Saha, U. K., "Sloshing of Liquids in Partially Filled Tanks – A Review of Experimental Investigations." Ocean Systems Engineering, 1(2), 131-15, 2011.

Eswaran, M., Singh, A., Saha, U. K., "Experimental Measurement of the Surface Velocity Field in an Externally Induced Sloshing Tank." Proc.IMechE, Part M: Journal of Engineering for the Maritime Environment, 225, 133-148, 2011.

Fukaya, M., Madarame, H., and Okamoto, K., "Growth Mechanism of Self-Induced Sloshing Caused by Jet in Rectangular Tank." (2nd report, multimode sloshing caused by horizontal rectangular jet). Trans. JSME, Ser. B, 62(599), 64–71, 1996.

Graczyk, M. Moan, T., and Rognebakke, O., "Probabilistic Analysis of Characteristic Pressure for LNG Tanks." J. Offshore Mech. Arct.,128(2), 133-144, 2006.

Hu H., Kobayashi, T., Saga, T., Segawa, S., and Uemura, T., "A PIV Study on the Self-Induced Sloshing Phenomena in a Rectangular Tank." Proc. of the '99 Korea–Japan Joint Seminar on Particle Image Velocimetry, 132–139., 1999.

Ibrahim, R. A., "Liquid Sloshing Dynamics: Theory and Applications." 1st edition, Cambridge University Press, New York, 2005.

Kimura, K., Ogura, K., Mieda, T., Yamamoto, K., Eguchi, Y., Moriya, S., Hagiwara, Y., Takakuwa, M., Kodama, T. and Kolke, K., "Experimental and Analytical Studies on the Multi-surface Sloshing Characteristics of a Top Entry Loop Type FBR." Nuclear Engineering Design, 157(1-2), 49-63, 1995.

Kline, S. J., and McClintock, F. A., "Describing Uncertainties in Single-sample Experiments." Mechanical Engineering, 75, 3–8, 1953.

Law, C. N. S., Khoo, B. C., and Chew, T. C. "Turbulence Structure in the Immediate Vicinity of the Shear-free Air–water Interface Induced by a Deeply Submerged Jet." Experiments in Fluids, 27, 321–331, 1999.

Lee, S.J., Kim, M.H., Lee, D.H., Kim, J.W. and Kim, J.H. "The Effects of LNG-tank Sloshing on the Global Motions of LNG Carriers." Ocean Engineering, 34(1), 10–20, 2007.

Maleki, A., and Ziyaeifar, M., "Sloshing Damping in Cylindrical Liquid Storage Tanks with Baffles." Journal of Sound and Vibration, 311, 372–385, 2008.

Nasar, T., Sannasiraj, S. A., and Sundar, V., "Wave Induced Sloshing Pressure In a Liquid Tank Under Irregular Waves." Proc. IMechE, Part M: J. Engineering for the Maritime Environment, 223(2), 145–161, 2009.

Okamoto, K., Madrarame, H., and Hagiwara, T., "Self-induced Oscillation of Free Surface in a Tank with Circulating Flow." Proc. of the IMechE Conference, Paper C416/092, 539–545, 1991.

Okamoto, K., Fukaya, M., and Madarame, H. "Self-Induced Sloshing Caused By Flow In A Tank." Proc. of the ASME Pressure Vessels and Piping Conference, 258, 105–111, 1993.

Pal, N. C., Bhattacharyya, S. K., and Sinha, P. K., "Non-linear Coupled Slosh Dynamics of Liquid-filled Laminated Composite Containers: a Two Dimensional Finite Element Approach." Journal of Sound and Vibration, 261(1), 729–749, 2002.

Panigrahy, P. K., Saha, U. K., and Maity, D. "Experimental Studies on Sloshing Behavior due to Horizontal Movement of Liquids in Baffled Tanks." Ocean Engineering, 36(3–4), 213–222, 2009.

Saga, T., Hu, H., Kobayashi, T., Murata, S., Taniguchi, S., Okamoto, K., and Nagoshi, M. A, "Comparative Study of the PIV and LDV Measurements on a Self-Induced Sloshing Flow." Journal of Visualization, 3(2), 145–156, 2002.

Singh, A., Nir, A., and Semiat, R, "Free-Surface Flow of Concentrated Suspensions." International Journal of Multiphase Flow, 32(7), 775–790, 2006.

Takizawa, A., Koshizuka, S., and Kondo, S., "Generalization of Physical Components Boundary Fitted Coordinate (PCBFC) Method For The Analysis Of Free Surface Flow." International Journal of Numerical Methods in Fluids, 15, 1213–1237, 1992.

APPENDIX - Error Analysis

Measured Quantities

TABLE A1 MAXIMUM POSSIBLE UNCERTAINTY FOR MEASURED QUANTITIES

Sl No	Measurement	Device	Accuracy	Minimum Quantity	Maximum Uncertainty
1	Time	Stop Watch	± 0.5 s	120 s	± 0.5 %
2	Pressure	Piezo-resistive type transducer	± 0.01bar	5 bar	± 0.2 %
3	Wave height	Capacitance wave gauge	± 0.2 mm	0.05m	± 0.4%

In this experimental investigation the parameters time, pressure and liquid height are measured quantities. Stop watch is used to measure time and piezo-resistive sensor is used for pressure analysis. During motion of the tank, the liquid height is measured by interface location technique and traditional wave height gauge.

Estimated Quantities

The frequency parameter is estimated from the number of cycles completed per second. Here, the uncertainty is calculated as $\frac{\Delta F}{F} = 0.42\%$ using the procedure described by Kline and McClintock (1953).

Dr. M. Eswaran received his PhD in Mechanical Engineering from Indian Institute of Technology Guwahati, India in 2011. Currently, he is working as a research associate in Bhaba Atomic Research Centre, Trombay, Mumbai, India under KSKRA Fellowship Scheme. He has published several technical papers in international journals, and conferences. His broad areas of research interest include slosh dynamics, fluid structure interactions, computational and experimental fluid dynamics.

Dr. U. K. Saha received his PhD in Aerospace Engineering from Indian Institute of Technology Bombay, India in 1996. Currently, he is a Professor in the Department of Mechanical Engineering, Indian Institute of Technology Guwahati. His broad areas of research include internal combustion engines, wind energy, compressor aerodynamics, propulsion and slosh dynamics. He has so far published 33 technical papers in international journals and 40 papers in international conferences. He is often being invited as a reviewer of many international journals and conferences. He has supervised several R & D and consultancy projects. He is an ASME member.